

# Architecture of floral branch systems in maize and related grasses

Erik Vollbrecht<sup>1†</sup>, Patricia S. Springer<sup>1†</sup>, Lindee Goh<sup>1†</sup>, Edward S. Buckler IV<sup>2</sup> & Robert Martienssen<sup>1</sup>

**The external appearance of flowering plants is determined to a large extent by the forms of flower-bearing branch systems, known as inflorescences, and their position in the overall structure of the plant. Branches and branching patterns are produced by tissues called shoot apical meristems. Thus, inflorescence architecture reflects meristem number, arrangement and activity, and the duration of meristem activity correlates with branch length. The inflorescences of maize, unlike those of related grasses such as rice and sorghum, predominantly lack long branches, giving rise to the tassel and familiar corncob. Here we report the isolation of the maize *ramosa1* gene and show that it controls inflorescence architecture. Through its expression in a boundary domain near the nascent meristem base, *ramosa1* imposes short branch identity as branch meristems are initiated. A second gene, *ramosa2*, acts through *ramosa1* by regulating *ramosa1* gene expression levels. *ramosa1* encodes a transcription factor that appears to be absent in rice, is heterochronically expressed in sorghum, and may have played an important role in maize domestication and grass evolution.**

Inflorescence architecture comprises the stereotypical number and arrangement of floral branches that characterizes each species of flowering plant<sup>1,2</sup>. The presence or absence of long branches, for example, dictates the capacity for flower production. Therefore, in grasses including the domesticated cereals, branch length greatly affects grain-bearing capacity. Grass flowers are always produced on a specialized short branch called the spikelet, so that architecture in grasses is largely determined by iterations of branching before spikelet production, by whether or not branch primordia grow out, and by axis orientation in space<sup>3,4</sup>. Branch length is central because of its macroscopic ramifications. The head of wheat, for instance, bears spikelets directly on the principal axis and thus appears quite different from a long branched inflorescence like that of rice.

Maize possesses a canonical grass architecture and two types of inflorescences, the tassel and the ear (Fig. 1), which differ in the presence of long, indeterminate (that is, bearing a large number of parts) branches at the tassel base<sup>5,6</sup>. Otherwise, the ear and the upper tassel develop from morphologically similar spikes. The spike primordia bear many short, determinate (that is, having a fixed number of parts) branches; each short branch is called a spikelet pair because it bears two spikelets. The classical mutants *ramosa1* (*ra1*) and *ramosa2* (*ra2*) have long instead of short inflorescence branches. *ramosa1* was discovered in a farmer's field almost a century ago<sup>7</sup> and has a branched, conical inflorescence (Fig. 1b, e) like that of many other grasses. Unlike other inflorescence mutants<sup>8</sup>, *ramosa1* is fully fertile and was initially classified as a new species, *Zea ramosa*<sup>7,9</sup>, although it corresponds to a recessive mutation at a single locus on chromosome 7 (ref. 10). We isolated the *ra1* gene from maize and its close relatives, and from species in the sugar cane tribe, for which the last common ancestor with maize lived some 16 million years ago. Our findings address the genetic origins of the maize ear, suggest a general role for the *ramosa* genes in long-branch architecture in cereals, and implicate the *ramosa* pathway in the evolutionary diversification of grass inflorescence development.

## ***ramosa1* encodes a transcription factor**

During maize inflorescence development, the apex initiates successive primordia that mature as they are displaced towards the base<sup>11</sup>. Thus, a chronology of developmental stages can be observed with a scanning electron microscope (SEM), from youngest at the apex to oldest at the base. In normal tassels, the primary inflorescence meristem initiated a few second-order meristems that were indeterminate (green arrowheads in Fig. 1h, i), and then switched to producing only determinate second-order meristems (red arrowheads in Fig. 1h, i). All second-order meristems in ears were determinate, producing paired spikelets (Fig. 1j) and straight, paired rows of kernels (Fig. 1d). In *ra1-R* mutants, no extra branch initiation was observed, but second-order meristems continued to grow into protruding second-order axes (Fig. 1m, n) that developed directly into the extra, long and indeterminate branches of mature mutant ears and tassels (Fig. 1o, p). Thus, the *ra1* gene imposes a determinate fate on second-order meristems.

To clone *ra1*, we used *Suppressor-mutator* (*Spm*) transposable elements in a directed transposon-tagging strategy<sup>12</sup>. Three recessive alleles were recovered with somatically unstable (that is, mutable) inflorescence phenotypes (Fig. 1c, f), a hallmark of transposon-induced mutations. Genetic experiments with two alleles, *ra1-m2* and *ra1-m3*, identified tight linkage between the mutable phenotype and an autonomous *Spm* transposon (see Supplementary Information). Molecularly, these were independent *Spm* insertions that were not present in their progenitor chromosome (for example, Fig. 2a). We cloned DNA adjacent to *Spm* on the *ra1-m2* chromosome and used it to discover that the *ra1-m3* chromosome contained a different *Spm*, inserted 188-bp away. Plants with sectored tassels were mosaic for the *Spm* insertion, and the element was absent from *ra1-m* loci that had changed to stably mutant alleles (Fig. 2a). Two other alleles, *ra1-m1* and *ra1-m4*, also contained *Spm* insertions, all within a 690-bp window, identifying the *ra1* locus.

Plants with mutable phenotypes were chimaeras for *Spm* insertions,

<sup>1</sup>Cold Spring Harbor Laboratory, Cold Spring Harbor, New York 11724, USA. <sup>2</sup>USDA, ARS and Department of Plant Breeding, Cornell University, Ithaca, New York 14850, USA.

†Present addresses: Department of Genetics, Development and Cell Biology, Iowa State University, Ames, Iowa 50011, USA (E.V.). Department of Botany and Plant Science, Center for Plant Cell Biology, University of California, Riverside, California 92521, USA (P.S.). The Boston Consulting Group, 1 Exchange Place, Boston, Massachusetts 02109, USA (L.G.).

which was useful for inferring some aspects of *ra1* function. Clonal tassel sectors were scored as revertant (phenotypically normal) if a row of determinate second-order meristems was flanked by a row(s) of indeterminate second-order meristems. Pollen is derived from the inner cell layer (L2) in maize<sup>13</sup>, so we used pollen from individual flowers within revertant sectors to compare the genotypes of inner tissue layers with sector phenotype. In one example, pollen from only one of four narrow sectors (between four and ten spikelets long) transmitted the revertant allele. So the other three sectors were phenotypically normal even though their L2 cells were mutant. Therefore, transposon excision in other cells, such as the outer L1 layer, provided *ra1* activity that conferred determinacy. Similarly, large revertant sectors in the ear imposed determinacy on genetically mutant second-order meristems at sector boundaries (Fig. 1f). Thus, *ra1* functions cell-nonautonomously.

The transposon insertions interrupted a gene encoding a Cys<sub>2</sub>-His<sub>2</sub>

zinc-finger protein belonging to the plant-specific EPF subclass<sup>14</sup>. The EPF zinc-finger binds DNA via a short  $\alpha$ -helix containing the amino acid sequence QALGGH<sup>14</sup>, which is conserved invariantly in the 28 and 33 single-finger EPF genes of *Arabidopsis* and rice, respectively. The *ra1* gene in maize and its orthologues in other grasses encode the variant QGLGGH (with a helix-relaxing Gly residue instead of Ala), suggesting that the RA1 zinc-finger may have unique functional attributes (Fig. 2d). Neither *Arabidopsis* nor rice appear to contain an orthologous gene (see Methods), but the most similar *Arabidopsis* EPF gene is *SUPERMAN*, which represses supernumerary stamens and is expressed in a boundary domain of floral meristems<sup>15</sup>. Strong mutant alleles *ra1-TN* and *ra1-R* contained point mutations in absolutely conserved residues in the zinc-finger (C51Y and H64N, respectively) and are probably null alleles<sup>15</sup>; weak alleles contained altered amino- and carboxy-terminal amino acid sequences (Fig. 2c). *ra1* RNA was detected only in developing inflorescences. The strong point mutant *ra1-R* and two weak alleles showed unaltered RNA

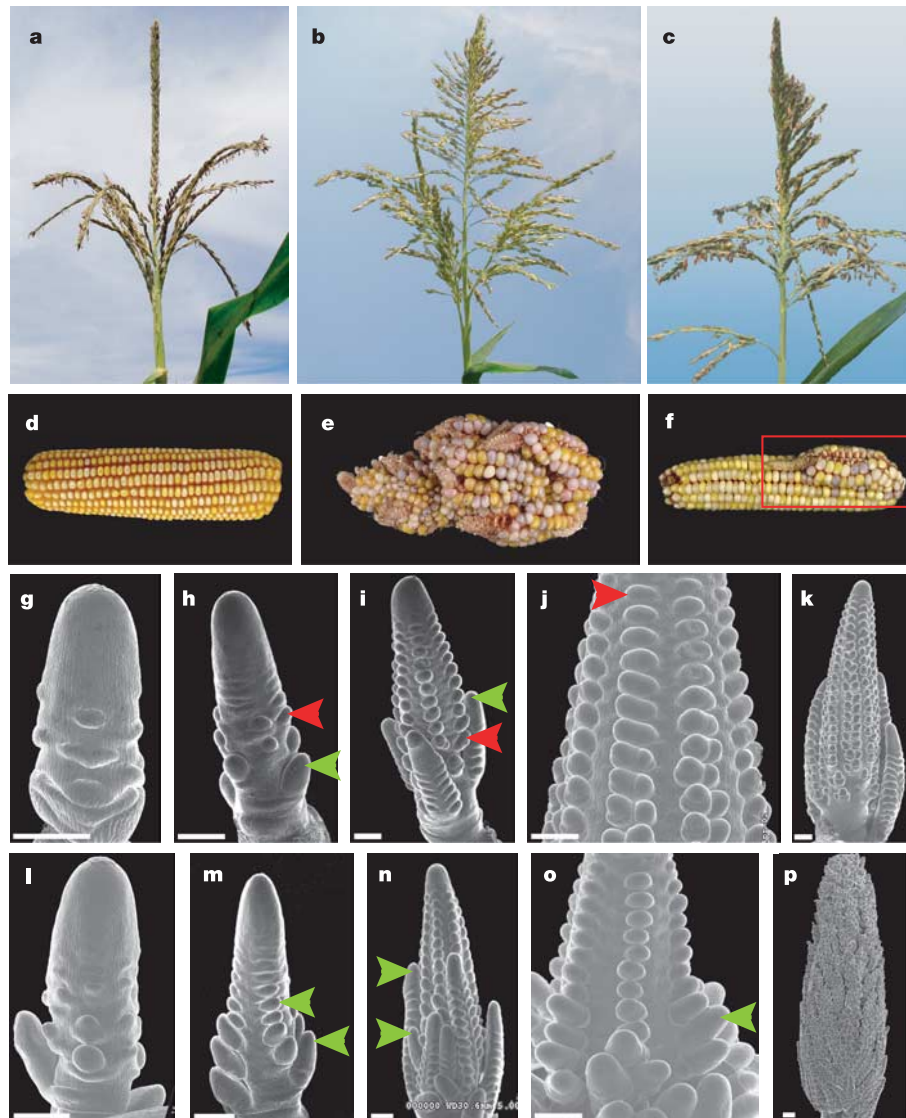


**Figure 1 | Maize inflorescences.** **a, d,** Normal tassel and ear. **b, e,** Mutant, highly branched *ra1-R* tassel and ear. **c, f,** Mutant *ra1-m2* tassel and ear are mosaics of normal and mutant tissue. The mutant ear sector (red box) contains spotted kernels and therefore *Spm* transposon activity. The zone of spotted kernels extends beyond the sector boundary into the normal portion. **g–k,** Scanning electron micrographs of tassel (**g–i, k**) and ear (**j**)

development in standard inbred B73 maize. Most second-order meristems in the tassel (for example, red arrowhead in **h**) and all secondary meristems in the ear (**j**) produce short, compact branches. **l–p,** Developing *ra1-R* tassel (**l–n, p**) and ear (**o**). Most second-order meristems in the tassel (green arrowheads in **m**) and in the ear (**o**) produce transformed, long branches. Scale bars, 250  $\mu$ m.



slightly later, when *ra1* was expressed on the lower (abaxial) edge of the differentiating third-order branch (spikelet) (Fig. 3c).

The early *ra1* expression domain suggested either that *ra1* marks the persistent second-order meristem until it initiates third-order meristems or that *ra1* transiently marks a boundary between indeterminate and determinate branch axes. In the normal inflorescence, the spikelet pair (second-order) meristem remains close to the primary axis, making it difficult to distinguish between these hypotheses (Fig. 3d). We therefore examined *ra1* expression in strong *ra1-R* mutants, in which axis growth carries second-order meristems away from the primary axis. As second-order meristems initiated, the *ra1-R* transcript was detected in the normal, adaxial domain. After the indeterminate second-order meristem was borne away from the axis, expression persisted at the junction between second-order meristems and the primary axis (Fig. 3e). Expression in *ra2-R* mutants was reduced (Fig. 3f), as discussed below. Thus, *ra1* imposes determinacy on nascent second-order meristems, not in the meristem *per se*, but in a boundary domain near the junction with the indeterminate primary axis.

Traversing from base to apex, the main axis of wild-type tassels (Fig. 4a) bore first long and then strictly short spikelet pair branches (Fig. 4k, bottom and top panels). Strong *ra1-R* mutants (Fig. 4d) first produced a few extra long branches bearing spikelet pairs (Fig. 4j, green), followed by several transformed, mixed-fate branches bearing both spikelet pairs and single spikelets (Fig. 4j, yellow). Proceeding apically, transformed branches bore multiple, single spikelets (Fig. 4j, orange). Successive spikelet multimers bore progressively fewer spikelets until they occurred strictly in pairs, defining a short, apical spike. Normal tassels produced simple, long branches at their base (Fig. 4a), but strong mutants produced compound, branched side axes (Fig. 4d) bearing a similar range of transformed branch fates as the main axis. Thus, second-order meristems that lacked *ra1* boundary function adopted a relatively continuous range of fates, revealing an underlying apical–basal gradient of indeterminacy.

Weak *ra1-RS* mutants (Fig. 4c) produced the same range and relative arrangement of altered second-order branch fates as strong mutants, but transition types occurred across a smaller region, resulting in a longer apical spike (Fig. 4j). This constricted transition region indicates a threshold-dependent interaction, in which second-order branch determinacy is controlled by the interplay of *ra1* boundary activity (allele strength) and position in an apical–basal gradient.

#### A genetic pathway regulates inflorescence branching

*ramosa2* (*ra2*) and *liguleless2* (*lg2*) mutants have more (Fig. 4b) or fewer (Fig. 4e) long branches in the inflorescence, respectively<sup>16,17</sup>. Using SEM, we observed that in *ra2-R* mutants, extra long branches developed directly from transformed, indeterminate second-order meristems (not shown), and resembled those in weak *ra1* mutants (Fig. 4j). Inbred B73 maize produces a compact ear with straight rows of kernels (Fig. 4l). In B73, *ra2-R* and weak *ra1-RS* mutants each produced fertile ears with crooked rows owing to slight second-order branch indeterminacy (Fig. 4m, n), whereas strong *ra1-R* mutants produced highly branched, functionally sterile ears (Fig. 4o). Notably, *ra2-R*;*ra1-RS* double mutants produced highly branched ears (Fig. 4p) that resembled those of *ra1-R* (strong) mutants. We therefore examined *ra1* expression in *ra2-R* mutants. RNA gel blots indicated that it was considerably reduced (data not shown), consistent with RNA *in situ* hybridizations in which *ra1* was expressed in its normal position at the base of second-order meristems, but in a highly constricted domain that appeared as a small speck (Fig. 3f). Thus, *ra2* regulates accumulation of *ra1* transcripts, placing the two genes in a single (*ramosa*) genetic pathway, with *ra2* upstream of *ra1*.

In *lg2-R* mutants, long branches at the base of the tassel failed to initiate and were replaced by bare nodes<sup>17</sup> (Fig. 4e, g, j). Thus, *lg2* function is required for either identity or outgrowth of these long branches. To distinguish between these possibilities, we constructed double mutants of *lg2-R* and each strong *ramosa* mutation, *ra1-R* and

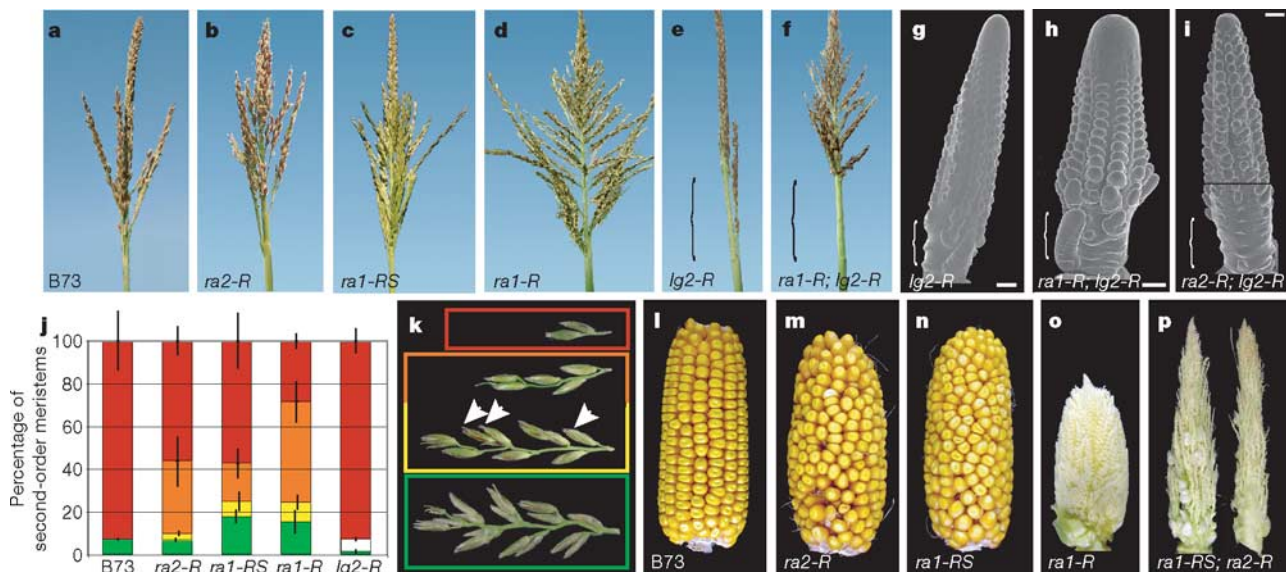


**Figure 4 | Developmental genetics of long branch pathways.** All alleles are in the maize inbred B73 (a, l) genetic background. b–d, *ra2-R* (b), weak *ra1-RS* (c) and strong *ra1-R* (d) mutant phenotypes. e, *lg2-R* mutants form bare nodes instead of basal branches (bracketed region). f, Additive phenotype of *ra1-R*;*lg2-R* double mutant separates *lg2* and *ra1* pathways. g–i, Scanning electron micrographs of immature tassels. Bare nodes of all mutants containing *lg2-R* have the same developmental basis: failure to initiate or maintain second-order meristems. j, k, Apical–basal distribution of tassel second-order meristems that developed as canonical, determinate spikelet

pairs (red; top panel in k), slightly indeterminate ‘spikelet multimer’ branches (orange; upper middle panel in k), mixed, indeterminate long branches bearing single (arrow) and paired (double arrow) spikelets (yellow; lower middle panel in k), and canonical, indeterminate long branches that bear spikelet pairs (green; bottom panel in k). White box indicates bare nodes. Error bars indicate standard deviation of the class below. l–p, Mature ears. *ra2-R* (m) and *ra1-RS* (n) have similar, weak phenotypes. The double mutant ear (p) is highly branched, like *ra1-R* (o), implying that *ra1* and *ra2* affect the same determinacy process. Scale bars, 250  $\mu$ m.

*ra2-R*. Both double mutants produced tassels with bare nodes basally, and transformed, long branches apically (Fig. 4f, h, i). Thus, *Ig2* is specifically required for branch outgrowth only at the base of the tassel, defining a distinct genetic pathway that regulates long branching upon the transition to flowering<sup>17</sup>.

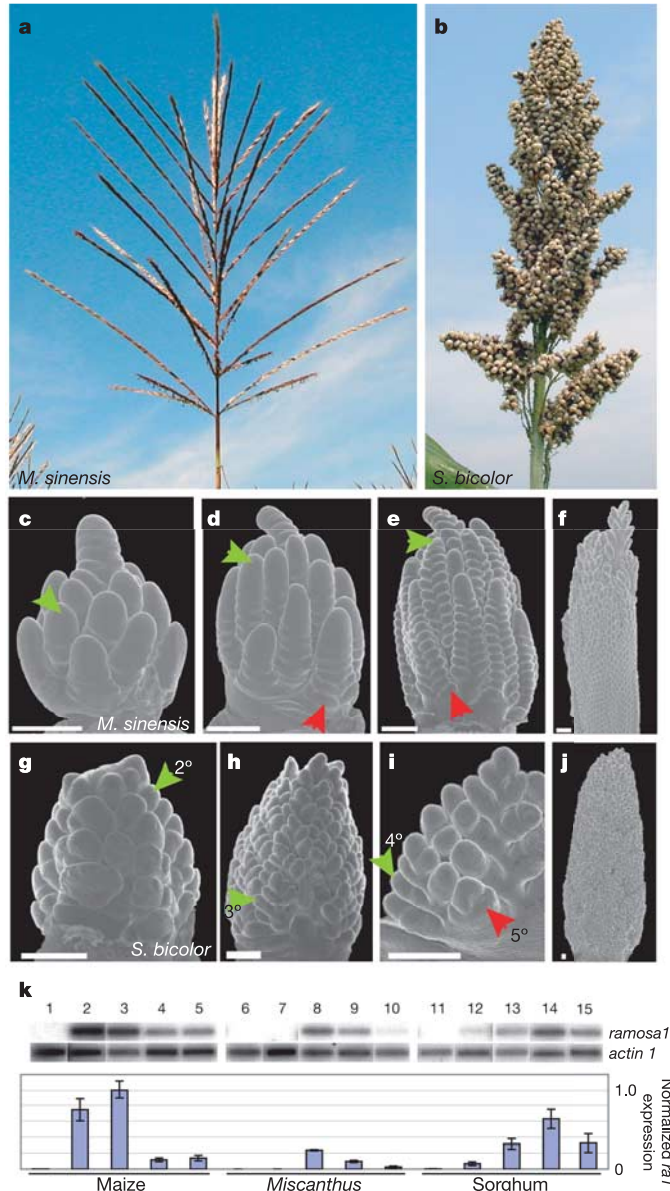


**Figure 5 | Comparative development and *ra1* expression in Panicoid grasses.** **a, b**, Mature inflorescences. *Miscanthus sinensis* (**a**) is moderately branched like maize, *Sorghum bicolor* (**b**) is reiteratively branched like maize *ramosa* mutants. **c–f**, Scanning electron micrographs of *M. sinensis* development. All second-order meristems ( $2^\circ$ ) are indeterminate (**c, d**, green arrows) and all third-order meristems ( $3^\circ$ ) are determinate (**d, e**, red arrows) and produce spikelet pairs. **g–j**, *S. bicolor* development. Multiple orders of indeterminate branching occur (**g–i**, green arrows) before fifth-order meristems (**i**, red arrow) typically become spikelet pairs. **k**, Semi-quantitative RT–PCR of *ra1* gene expression, showing raw data (above) and *ra1* normalized to *actin1* levels (below). RNA was isolated from vegetative apices (lanes 1, 6 and 11), carefully staged tassels of B73 (lanes 2–5), and analogous stages of *Miscanthus* (7–10) and sorghum (12–15) that match **c–f** and **g–j**, respectively. The abrupt transition from indeterminate to determinate second-order meristems in maize and *Miscanthus* is accompanied by an abrupt onset of *ra1* gene expression. In sorghum, delayed production of spikelet pairs correlates with a protracted onset of *ra1* expression. Error bars indicate s.d. Scale bars, 250  $\mu$ m.

### The *ra1* pathway in grass evolution and domestication

Although maize normally produces spikelets only in pairs, mutants with different levels of *ra1* activity produce long branches and spikelet multimers, resembling architectures of other grasses<sup>18</sup>. The popular ornamental grass *Miscanthus sinensis* produces a visually simple inflorescence with discrete, long branches (Fig. 5a), similar to the base of the maize tassel. The crop plant *Sorghum bicolor*, on the other hand, generates a dense, multi-branched head (Fig. 5b) that resembles a *ramosa* mutant. We isolated the *ra1* orthologue from each species (Fig. 2d). In maize, *ra1* expression was highest when second-order meristems were initiated, imposing determinacy on these spikelet pairs. Expression dropped off suddenly as third- and higher-order meristems were produced on spikelet pair axes (Fig. 5k, lanes 1–5). During *Miscanthus* development, all second-order meristems were indeterminate (green arrows in Fig. 5c–e). This extended phase of indeterminate second-order meristems correlated with a delayed, similarly narrow window of *ra1* expression (Fig. 5k, lanes 6–10), which was highest when strictly determinate third-order meristems became spikelet pairs (red arrows in Fig. 5d, e) and then dropped off as fourth- and higher-order meristems were produced on spikelet pair axes. Thus, maize and *Miscanthus* showed similar expression dynamics, reflecting similar architectures in which spikelet pairs are all produced from a single order of meristem. Expression dynamics differed for sorghum, in which all second-, most third- and even fourth-order meristems were indeterminate (Fig. 5g–i), such that spikelet pairs were derived from third- to fifth-order meristems. The late acquisition of spikelet pair fate in sorghum, together with the continual indeterminate branching and extended phase of *ra1* expression (Fig. 5k, lanes 11–15), suggest that *ra1* activity reaches a threshold level sufficient to impose determinate spikelet pair fate at a relatively late developmental stage. Thus, *ra1* activity regulates long branch architecture similarly in these three species, by imposing spikelet pair identity on the appropriate order of meristem.

A gene that regulates natural inflorescence diversity in the grasses might be a target for selection during the domestication of a crop species like maize, in which the ear inflorescence has undergone such intense selective pressure as to be regarded a monstrosity relative to typical wild species<sup>19</sup>. We surveyed the sequence of the *ra1* locus in a panel of diverse, inbred strains of maize, which had previously been examined for multiple loci that have or have not undergone selection<sup>20</sup> (see Supplementary Information). Silent site diversity at *ra1* ( $\pi = 0.0010$ ) was  $>10$ -fold less than that of typical, non-selected maize genes ( $\pi = 0.0107$ ), but  $>2$ -fold lower than observed for starch pathway genes ( $\pi = 0.0027$ – $0.0050$ ), which were targets of human selection during maize domestication and improvement<sup>20</sup>. We tested for selection at *ra1* using Hudson–Kreitman–Aguadé (HKA) tests<sup>21</sup>, which were highly significant ( $P < 0.0001$ ). These data all indicate that *ra1* was a target of positive directional selection in the maize lineage. Consistent with selection, the diverse inbreds contained only three haplotypes at *ra1*, and we detected no evidence for recombination. Such low recombination is uncommon in maize<sup>22–24</sup>.

### Discussion

The plant morphologist W. Troll surveyed some 40,000 species to infer that the flowering plant shoot is comprised of zones defined by branch determinacy and their relationship to the parent shoot<sup>25</sup> (Fig. 6): the E zone (final inflorescence), the subapical ZE (zone of inflorescence enrichment), the INZ (zone of inhibition) and the basal IZ (innovation zone of renewal growth). Conspicuous in the transition from vegetative to inflorescence shoot is the precocious outgrowth of lateral meristems, so that the ZE usually contains many side branches (paracladia) and the INZ relatively few. For all zones, paracladia repeat the morphology of the principal axis at their site of attachment—the lower the paracladium, the more extensive is the repetition. Thus, Troll's model considers the inflorescence in

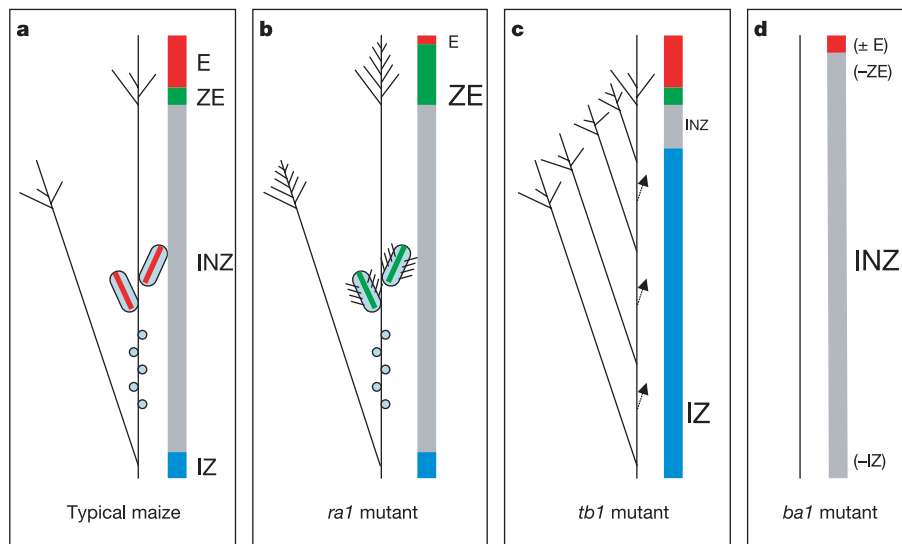


**Figure 6 | A model for heterochronic modulation of inflorescence and plant architecture.** **a**, Normal maize shoot (schematic) illustrates elements of Troll's holistic model (coloured bars on right): the shoot zones include the zone of innovation (IZ, blue bar), the zone of inhibition (INZ, grey bar) with ear shoots mostly unelaborated (small circles) and a few elaborated shoots (ovals), the zone of enrichment (ZE, green bar) and the final inflorescence (E zone, red bar). Paracladia in IZ and ZE mimic their parent shoot above the

point of origin. **b–d**, For mutants, only affected zones are labelled; altered font size reflects enlarged or contracted zones. **b**, *ra1-R* mutants expand the ZE at the expense of the E zone. **c**, *tb1* mutants expand the IZ into the INZ (only one half of the *tb1* shoot is shown). **d**, Depending on the allele strength, *ba1* mutants expand the upper INZ to eliminate the IZ and ZE entirely, and decrease the length of the E zone.

the context of the whole shoot system. In maize, for example, tillers in the basal IZ reproduce the entire plant, but higher lateral branches are short and tipped by an inflorescence (the ear) that mimics just the E zone of the tassel. Except for basal long branches in the tassel, the majority of the ZE is suppressed by *ra1* so that a 'determinacy gradient' is only evident in the absence of *ra1* function. In the ear branch, this suppression affords the remarkable packing of kernels in the corn cob.

Each of the zones envisioned by Troll arises in a fixed temporal sequence, with later structures at the apex and earlier ones at the base. Thus, genes such as *ra1* that suppress elaboration of a given zone may be considered heterochronic: *ra1* accelerates later stages of branch development (spikelet pairs) at the expense of earlier ones (long branches). The gradation of mutant branch types, and the shift in this gradation with allele strength, mimics altered temporal transitions of other heterochronic mutations in maize<sup>26</sup>. Changes in the developmental timing of *ra1* expression, attributable for example to promoter rearrangements at *ra1* or to alterations in *ra2*, underlie a difference in inflorescence architecture in certain maize alleles as well as in related grasses. A similar model can be proposed for modulation of earlier zones by *teosinte branched1* (*tb1*) and *barren stalk1* (*ba1*), which regulate multiple lateral meristems in vegetative and reproductive shoots, respectively, and modulation of later zones by *indeterminate spikelet1* (*ids1*) and *branched silkless1* (*bd1*)<sup>8,27–29</sup>. *lg2* has also been described as heterochronic<sup>17</sup>. Interestingly, these genes all encode transcription factors. Moreover, *ra1*, *ba1* and *bd1* are all expressed in boundary domains adjacent to the meristems they regulate, and *ra1* (at least) displays cell-nonautonomy. The products of these genes may affect zones by regulating a mobile signal for meristem determinacy, or be mobile themselves. Other genes affect inflorescence architecture without modifying temporal zones, for example by regulating meristem size (for example, *fasciated ear2*, *thick tassel dwarf1* and *knotted1*<sup>30–32</sup>).

Almost a century ago, the similarity of *ra1* mutants to other grasses led to the proposal that *ra1* represented a 'revertant' or atavistic evolutionary form<sup>33</sup>. Our data indicate directional selection for a narrow set of *ra1* alleles, either during maize domestication from its wild ancestor teosinte or during agricultural improvement in the

subsequent 9,000 yr. We propose that selection was most likely for suppressed branching in the ear. Modern inbreds never have long-branched cobs, yet they are diverse for tassel branch number. Furthermore, although the tiny, two-rowed teosinte ear is also unbranched, it is highly divergent from its massive, modern maize counterpart. Ear improvement probably involved selecting genes that increased the size of primary meristems<sup>30</sup>, which in turn produced more second-order meristems and may have intensified a requirement to keep second-order meristems determinate. The selected trait is probably also still variable in extant teosinte, so we predict that teosinte *ra1* alleles will be more diverse molecularly, and perhaps even phenotypically, when introduced into maize. Key morphological differences between maize and teosinte can be accounted for by genetic changes in five major chromosomal regions; these include *tb1* and possibly *ba1*<sup>27,34,35</sup>, which are highly conserved in sequence and function across most of the grass phylogeny<sup>27,36</sup>. Such purifying selection is expected to constrain the ability of *tb1* and *ba1* to confer evolutionary novelty. However, domestication was a complex process that acted on an enormous number of traits and their controlling genes<sup>37</sup>. *ra1* is not within the five regions, and regulates a specific meristem determinacy switch<sup>9</sup>, the implementation of which varies even between relatively closely related species. Moreover, *ra1* sequence diverges rapidly among these species, and the gene appears to be absent in distantly related rice, for which spikelet-bearing axes are indeterminate. Thus, *ra1* may function in the evolution of developmental diversity<sup>38,39</sup> and be useful for molecular breeding and crop development.

## METHODS

**Maize genetics and *ra1* gene cloning.** For transposon tagging, *o2*<sup>m20</sup>::*Spm* ears were fertilized with *ra1-R o2 gl1* pollen and the progeny were screened at maturity for branched tassels and ears. Three mutable alleles, *ra1-m1*, *ra1-m2* and *ra1-m3*, were identified among approximately 50,000 plants. *ra1-m4* was isolated from 20,000 plants from a cross between *bz1-mum9* ears and *ra1-R o2 gl1;sh1 bz1 wx1* pollen. All four alleles were caused by insertion of the *Spm* transposable element (see Supplementary Information), and a co-segregating DNA fragment from the *ra1-m2* allele was isolated by size-selecting *EcoRI*-digested DNA in an agarose gel and ligating into a  $\lambda$ -ZAP vector (Stratagene). Approximately 50,000 plaques were screened by hybridization with an *Spm*

probe. The DNA insert in one positive clone was isolated and sequenced. Transcript ends were determined by rapid amplification of cDNA ends (RACE)<sup>40</sup> using total RNA isolated from young inflorescences with Trizol (Gibco). DNA from various inbred and mutant *ra1* alleles was amplified by polymerase chain reaction (PCR) using gene-specific primers (and with transposon-specific primers for *Spm* alleles, as guided by DNA gel blots) and then sequenced. RNA gel blots used 5 µg total RNA per sample; nucleic acid gel blots were performed as described<sup>32</sup>. Maize alleles used for expression analysis were first crossed between three and six times to inbred B73. Maize and *Sorghum bicolor* (cultivar Btx623) were grown outdoors or in a greenhouse. Seasonally harvested *Miscanthus sinensis* was grown on the Cold Spring Harbor Laboratory grounds. To isolate *ra1* from sorghum, we screened a bacterial artificial chromosome (BAC) library (CUGI) with a maize probe and subcloned and sequenced a 6-kb *XbaI* restriction fragment that contained the tandemly duplicated locus. The same region was PCR-amplified and directly sequenced from sorghum genomic DNA for verification. *ra1* was isolated from *Miscanthus* by PCR (primers RA\_35 AACGACGGATCACGCTGTGTGTC, and Sb\_1826\_AS TGGACTCTGTGCTGTTGTTGGA) and TA-cloned, and multiple clones were sequenced until an identical sequence was obtained from different clones. EPF genes in rice and *Arabidopsis* were identified by searching proteome databases (MATDB, <http://mips.gsf.de/proj/thal/db/> and Gramene, <http://www.gramene.org>) with blastp using the Cys<sub>2</sub>-His<sub>2</sub> region of RA1 and a cutoff *p*-value of 1, followed by manual elimination of false positives. Lack of a *ra1* orthologue in rice or *Arabidopsis* was concluded based on not finding a conserved protein with the QGLGGH motif or with sequence similarity other than in the highly conserved, short Cys<sub>2</sub>-His<sub>2</sub> and EAR motifs.

**Phenotype and RNA expression analysis.** All developmental, morphological and double mutant phenotype analyses of maize were on material converged for at least four generations into the inbred B73. For morphometrics (Fig. 4j), 6–8 mature tassels of each genotype were dissected, classifying every second-order branch. The number of second-order meristems in each class was averaged and normalized against the total average number of second-order meristems. The bare nodes of *lg2* mutant tassels may be undercounted, as they are difficult to score unambiguously other than by SEM. For SEM of all species, freshly dissected inflorescences were mounted on stubs in silver paint (Electron Microscopy Sciences) and examined in an S-3500N scanning electron microscope (Hitachi) at high vacuum, using 3–10 kV accelerating voltage and a secondary electron detector. For maize RNA *in situ* hybridizations, inflorescence primordia were dissected, vacuum infiltrated and fixed at 4 °C overnight in 4% formaldehyde, prepared fresh from paraformaldehyde (Sigma) in phosphate-buffered saline. *In situ* hybridizations were performed as described<sup>41</sup>. Semi-quantitative PCR with reverse transcription at *ra1* was performed with primers RA\_53 (GCCGCCAC AGGTAAGGTCG) and RA\_49 (GCCAGTCTAAGCTGAAGAT CCA). RT-PCR with primers specific for each sorghum repeat determined that the upstream copy is hardly (but detectably) transcribed at all stages tested, but RA\_53 did not amplify the upstream (untranscribed) copy at the annealing temperature used (63.5 °C). A 'grass actin' primer set was designed on the basis of actin expressed-sequence-tag (EST) sequences from maize, sorghum, barley, *Setaria italica* and rice (primers actin\_F GTMARCAACTGGGAYGACATGGA GAA and actin\_B ACRTCRCACTTCATGATRGAGTTGTABGT, where M, R, Y and B are standard degenerate nucleotide codes). PCR assays of 23, 25 and 27 cycles were processed by DNA gel blot and hybridization. A pair of cycles showing linear changes for both the actin gene and *ra1* was selected to quantify average expression levels using a Fuji phosphorimager.

**Nucleotide diversity analysis.** A 1.5-kb *ra1* fragment that includes the transcribed region plus ~400 bp upstream and downstream was isolated by PCR (primers RA\_48 TCAACGTGGTCAAAGTTGTGTGTG and RA\_36 CAAGGTG CACCCACAACATTGAC) and sequenced from a set of 30 maize inbred lines<sup>20</sup>. Sequence alignments were made in ClustalW and adjusted by eye. Nucleotide diversity statistics were calculated using DnaSP<sup>42</sup>. HKA tests with neutral loci that were sequenced in the same panel of inbreds were performed by the direct method in DnaSP using *Tripsacum dactyloides* (PI 595898) as an outgroup (primers RA\_28 CGTGGCTGATCTCAACATCTCAA and RA\_11 TGCACCTGC ACGTACCCATTGTAG), and scores were combined as previously described<sup>20</sup>. PCR products from *Tripsacum* were TA-cloned and multiple clones sequenced until an identical sequence was obtained from different clones.

Received 9 March; accepted 6 June 2005.

Published online 24 July 2005.

- Weberling, F. *Morphology of Flowers and Inflorescences* (Cambridge Univ. Press, Cambridge, 1989).
- Sussex, I. M. & Kerk, N. M. The evolution of plant architecture. *Curr. Opin. Plant Biol.* **4**, 33–37 (2001).
- Clifford, H. in *Grass Systematics and Evolution* (eds Soderstrom, T., Hilu, K., Campbell, C. & Barkworth, M.) 21–30 (Smithsonian Institution Press, Washington DC, 1987).
- Doust, A. N. & Kellogg, E. A. Inflorescence diversification in the panicoid "bristle grass" clade (Paniceae, Poaceae): evidence from molecular phylogenies and developmental morphology. *Am. J. Bot.* **89**, 1203–1222 (2002).
- McSteen, P., Laudencia-Chinguanco, D. & Colasanti, J. A floret by any other name: control of meristem identity in maize. *Trends Plant Sci.* **5**, 61–66 (2000).
- Veit, B., Schmidt, R. J., Hake, S. & Yanofsky, M. F. Maize floral development: new genes and old mutants. *Plant Cell* **5**, 1205–1215 (1993).
- Gernert, W. A new subspecies of *Zea mays* L. *Am. Nat.* **46**, 616–622 (1912).
- Chuck, G., Muszynski, M., Kellogg, E., Hake, S. & Schmidt, R. J. The control of spikelet meristem identity by the *branched silkless1* gene in maize. *Science* **298**, 1238–1241 (2002).
- Postlethwait, S. N. & Nelson, O. E. Characterization of development in maize through the use of mutants. I. The *polytypic* (*Pt*) and *ramosa-1* (*ra1*) mutants. *Am. J. Bot.* **51**, 238–243 (1964).
- Emerson, R., Beadle, G. & Fraser, A. A summary of linkage studies in maize. *Cornell Univ. Agric. Experiment Station Memoir* **180**, 3–83 (1935).
- Cheng, P. C., Greyson, R. I. & Walden, D. B. Organ initiation and the development of unisexual flowers in the tassel and ear of *Zea mays*. *Am. J. Bot.* **70**, 450–462 (1983).
- McClintock, B. Induction of instability at selected loci in maize. *Genetics* **38**, 579–599 (1953).
- Dawe, R. K. & Freeling, M. Clonal analysis of the cell lineages in the male flower of maize. *Dev. Biol.* **142**, 233–245 (1990).
- Takatsuiji, H. Zinc-finger proteins: the classical zinc finger emerges in contemporary plant science. *Plant Mol. Biol.* **39**, 1073–1078 (1999).
- Sakai, H., Medrano, L. J. & Meyerowitz, E. M. Role of SUPERMAN in maintaining *Arabidopsis* floral whorl boundaries. *Nature* **378**, 199–203 (1995).
- Nickerson, N. H. & Dale, E. E. Tassel modifications in *Zea mays*. *Ann. Mo. Bot. Gard.* **42**, 195–211 (1955).
- Walsh, J. & Freeling, M. The *liguleless2* gene of maize functions during the transition from the vegetative to the reproductive shoot. *Plant J.* **19**, 489–495 (1999).
- Kellogg, E. in *Grasses: Systematics and Evolution* (eds Jacobs, S. & Everett, J.) (CSIRO, Melbourne, 2000).
- Kellogg, E. A. Plant evolution: the dominance of maize. *Curr. Biol.* **7**, R411–R413 (1997).
- Whitt, S. R., Wilson, L. M., Tenaillon, M. I., Gaut, B. S. & Buckler, E. S. Genetic diversity and selection in the maize starch pathway. *Proc. Natl Acad. Sci. USA* **99**, 12959–12962 (2002).
- Hudson, R., Kreitman, M. & Aguade, M. A test of neutral molecular evolution based on nucleotide data. *Genetics* **116**, 153–159 (1987).
- Tenaillon, M. I. *et al.* Patterns of DNA sequence polymorphism along chromosome 1 of maize (*Zea mays* ssp. *mays* L.). *Proc. Natl Acad. Sci. USA* **98**, 9161–9166 (2001).
- Remington, D. L. *et al.* Structure of linkage disequilibrium and phenotypic associations in the maize genome. *Proc. Natl Acad. Sci. USA* **98**, 11479–11484 (2001).
- Wilson, L. M. *et al.* Dissection of maize kernel composition and starch production by candidate gene association. *Plant Cell* **16**, 2719–2733 (2004).
- Troll, W. *Die Infloreszenzen: Typologie und Stellung im Aufbau des Vegetationskörpers* (Fischer, Stuttgart, 1964).
- Poethig, R. Phase change and the regulation of shoot morphogenesis in plants. *Science* **250**, 923–930 (1990).
- Gallavotti, A. *et al.* The role of *barren stalk1* in the architecture of maize. *Nature* **432**, 630–635 (2004).
- Doebley, J., Stec, A. & Hubbard, L. The evolution of apical dominance in maize. *Nature* **386**, 485–488 (1997).
- Chuck, G., Meeley, R. & Hake, S. The control of maize spikelet meristem identity by the *APETALA-2*-like gene *indeterminate spikelet1*. *Genes Dev.* **12**, 1145–1154 (1998).
- Taguchi-Shiobara, F., Yuan, Z., Hake, S. & Jackson, D. The *fasciated ear2* gene encodes a leucine-rich repeat receptor-like protein that regulates shoot meristem proliferation in maize. *Genes Dev.* **15**, 2755–2766 (2001).
- Bommert, P. *et al.* *thick tassel dwarf1* encodes a putative maize ortholog of the *Arabidopsis* CLAVATA1 leucine-rich repeat receptor-like kinase. *Development* **132**, 1235–1245 (2005).
- Vollbrecht, E., Reiser, L. & Hake, S. Shoot meristem size is dependent on inbred background and presence of the maize homeobox gene, *knotted1*. *Development* **127**, 3161–3172 (2000).
- Collins, G. Hybrids of *Zea tunicata* and *Zea ramosa*. *Proc. Natl Acad. Sci. USA* **3**, 345–349 (1917).
- Doebley, J. & Stec, A. Inheritance of the morphological differences between maize and teosinte: comparison of results for two F<sub>2</sub> populations. *Genetics* **134**, 559–570 (1993).
- Wang, R. L., Stec, A., Hey, J., Lukens, L. & Doebley, J. The limits of selection during maize domestication. *Nature* **398**, 236–239 (1999).
- Takeda, T. *et al.* The *OstT1* gene negatively regulates lateral branching in rice. *Plant J.* **33**, 513–520 (2003).

37. Doebley, J. The genetics of maize evolution. *Annu. Rev. Genet.* **38**, 37–59 (2004).
38. Kellogg, E. A. Evolution of developmental traits. *Curr. Opin. Plant Biol.* **7**, 92–98 (2004).
39. Martienssen, R. The origin of maize branches out. *Nature* **386**, 443–444 (1997).
40. Sambrook, J. & Russell, D. W. *Molecular Cloning: A Laboratory Manual* (Cold Spring Harbor Laboratory Press, Cold Spring Harbor, 2001).
41. Jackson, D., Veit, B. & Hake, S. Expression of maize *KNOTTED1* related homeobox genes in the shoot apical meristem predicts patterns of morphogenesis in the vegetative shoot. *Development* **120**, 405–413 (1994).
42. Rozas, J. & Rozas, R. DnaSP version 3: an integrated program for molecular population genetics and molecular evolution analysis. *Bioinformatics* **15**, 174–175 (1999).

**Supplementary Information** is linked to the online version of the paper at [www.nature.com/nature](http://www.nature.com/nature).

**Acknowledgements** We thank T. Mulligan for plant care, Z. Lippman and C. Kopec for help with *in situ* hybridization and SEM, R. J. Schmidt for producing and sharing the *ra1-RS* allele, D. Jackson for discussions and V. Irish for commenting on the manuscript. E.V. was a DOE-Energy Biosciences postdoctoral fellow of the Life Sciences Research Foundation. L.G. was supported by the Cold Spring Harbor Undergraduate Research Program. Grant support was provided by the Agricultural Research Service of the USDA (to E.S.B.), the National Research Initiative of the USDA CSREES (to R.M.), and by the NSF Plant Genome Research Program (to E.S.B. and R.M.).

**Author Information** DNA sequences reported here have been deposited in GenBank under accession numbers AY957396–AY957399 and DQ013174–DQ013203. Reprints and permissions information is available at [npg.nature.com/reprintsandpermissions](http://npg.nature.com/reprintsandpermissions). The authors declare no competing financial interests. Correspondence and requests for materials should be addressed to R.M. ([martiens@cshl.org](mailto:martiens@cshl.org)).